



ISSN 2345 - 4997

# Determination of Strong Ground Motion Using Empirical Green's Function in Boroujerd- Silakhor Earthquake- March 31, 2006

Jamileh Vasheghani Farahani\*<sup>1</sup>, Mehdi Zare<sup>2</sup>

<sup>1</sup> Institute of Geophysics, Tehran University, Tehran, Iran.

<sup>2</sup> International Institute of Earthquake Engineering and Seismology (IIEES), Tehran, Iran.

\* Corresponding Author ([j\\_farahani@ut.ac.ir](mailto:j_farahani@ut.ac.ir))

**Article History:**  
Revised: Feb. 03, 2014

Received: Jan. 15, 2014  
Accepted: Feb. 08, 2014

Reviewed: Feb. 01, 2014  
Published: Feb. 14, 2014

## ABSTRACT

Earthquakes have always been an important cause of mortalities and property damage in Iran. In regions where there are few strong motion records, the simulation of earthquake waveforms can be an important source for strong ground motions prediction. Strong motion records are vital for earthquake engineering purposes and developing spectra for earthquake resistant designs. The simulated motions might be applied in the design of spectral development. One of the major methods in the strong motion simulation is the application of empirical Green's function. In this method, aftershocks are considered as Green's functions and the target event or main-shock is calculated by dividing the fault into smaller parts as subfaults (each of which is a point source) and by using the summation principle and time delay in the wave distribution of each subfault. Empirical Green's function method was first used by Hartzel, 1978. The present research is concentrated on the simulation of strong motions for Silakhor earthquake- March, 31 2006, with  $M_w = 6.0$ . The simulation of strong motions based on the aftershocks of Silakhor event, shows proper consistency between the simulated and the recorded main-shock which is due to the maximal motion and the spectral ordinates.

**Keywords:** Strong Ground Motion; Empirical Green's Function Method; Aftershocks, Silakhor.

## 1. INTRODUCTION

Recognizing the power of the earthquakes and how they affect the structures have always been great questions to designers to whom the building codes offer some answers.

The simplest way to estimate earthquake loads is to use equivalent static method; however, despite the popularity and common use of this method, it cannot precisely clarify the structures' behavior during an earthquake. In order to understand the reaction of the structures in each time step during the earthquake, accelerograph (velocity or displacement) time history should be used as the input load.

Since high qualified strong motion records are not still available for all regions, finding an effective solution to supply the request is necessary. Empirical Green's function (E.G.F) is an effective method in simulating strong ground motions.

The first successful attempt for theoretical calculation of strong motions was presented by Aki (1963) and Haskels (1969), using kinematics source

model, given by propagating the dislocation over a fault plane in an infinite homogeneous medium.

Another approach to synthesize strong motions was proposed by Hartzel (1978), utilizing observed seismograms from small events as Green's functions. Later methods proposed by Hadley and Helmlerer (1980) and Irikura and Muramoto (1982) in Japan, attempted to synthesize the main-shock motions using small shocks (foreshocks and aftershocks).

This paper will represent the application of Empirical Green's function method for simulating the strong motions recorded in Boroujerd- Silakhor earthquake in Iran- using the recorded aftershocks.

It is then intended to generate the synthetic ground motions for Lorestan region based on E.G.F. method. The accelerometric data, used in this study, are recorded in Iranian National Strong Motion Network. This network has recorded Iran's earthquakes since 1974 which have been maintained by the Building and Housing Research Center.

First, the methodology of E.G.F, used in this research is explained, and then the greatest strong motion or mainshock in Boroujerd- Silakhor

earthquake which occurred on March 31, 2006 is simulated.

**2. MATERIALS AND METHODS**

This approach uses real records of earthquakes (typically aftershocks) to calculate the effect of a target event. To understand what is happening in each part of a particular fault, its surface is divided into a grid within which the aftershocks are located. This was used as Empirical Green's Functions (EGF). The basic idea underlying Green's functions method is the assumption that at a certain observational area, the overall ground motions caused by a large earthquake is the sum of several moderate events. Indeed, the ground motions caused by instantaneous slip on an individual segment of a fault can be represented by a mathematical method called Green's function. Firstly, Hartzel (1978) proposed the use of small recorded earthquakes as EGF to calculate a larger earthquake, and later the technique was developed by several other researchers. Recently, this technique has been used in Europe to evaluate seismic hazard, the applied model is based on the one proposed by Hutching et al. (1997) using:

- A simple Kinematic rupture model to describe the source in predicting strong ground motions for the full time history.
- EGF to constrain propagation path and site response information.

It develops an exact solution to the representation relation which can be expressed as the summation of small earthquakes records (either empirical or synthetic Green's functions) that will be convoluted with an analytical solution for the slip function.

Here, strong ground motions are simulated based on the equation proposed by Irikura, (1986) to synthesize the acceleration motion. Irikura's revised expressing formula is:

$$U(x,t) = \sum_{i=1}^l \sum_{j=1}^m \frac{F_{ij}^s}{F_o^s} \cdot \frac{r_o}{r_i} u(x.,t-t_z) + \sum_{i=1}^l \sum_{j=1}^m \sum_{k=1}^{(n-1)n'} \frac{F_{ij}^s}{F_o^s} \cdot \frac{r_o}{r_i} \cdot \frac{\lambda}{n'} \cdot u(x.,t-t_z - \frac{(k-1)\tau}{n.n'})$$

where,  $n' = \frac{\tau}{dt}$ ,

$dt$  : Data recording interval,  $\tau$  : Rise Time

$$t_z = \frac{r}{v_s} + \frac{\xi_{ij}}{v_r}$$

$\xi_{ij}$  : Distance between rupture point and ij segment,  
 $v_s$  : Shear wave velocity,  $v_r$  : Rupture velocity.

The mentioned equations match with Target earthquake moment and are consistent with  $N^3$  records summation.

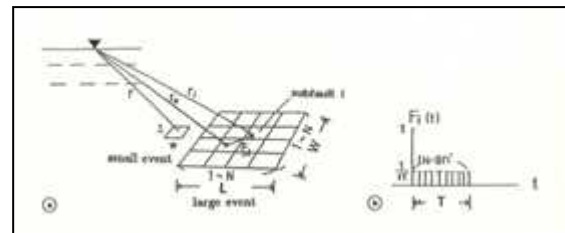


Fig 1. A) Schematic description of fault parameters used to calculate Green's experimental functions. The fault zone of the large and small events are shown as LxW and l'xw, respectively. B) Fi(t) is the filtration function for regulating the differences between the slip time functions of large events and those of small ones.

**2. 1. SILAKHOR EARTHQUAKE**

At 4:47:52 in the morning on March the 31<sup>th</sup> (2006), an earthquake of  $M_w = 6.0$  shocked the border between Borujerd and Dorood cities (Silakhor plain) in Lorestan province.

About 70 people were killed and over 2000 were injured. More than 300 villages were damaged seriously, overall. This earthquake was recorded by 15 digital accelerographs SSA-2 in Lorestan, Hamedan and Central provinces. The maximum accelerations were recorded in Chalanchoolan station with the peak values of about 439 and 522 cm/sec<sup>2</sup> on horizontal and vertical components, respectively. The recorded accelerogram in Chalanchoolan station is the closest obtained accelerogram.

**2. 2. IMPORTANT AND MAIN FAULTS OF THE REGION**

**2. 2. 1. ZAGROS MAIN THRUST:**

Zagros main thrust is one of the most important tectonic structures in Iran that plays an effective role in the structural tectonic evolutions. This thrust continues from the north of Bandar Abbas toward Marivan region and is 1350 km long. Tectonic motion studies show no evidence of high seismic activities of this fault and/ or of being the macro-seismic plane of a great earthquake.

**2. 2. 2. ZAGROS MAIN RECENT FAULT**

Zagros northwest border is on Zagros main reverse fault and Zagros main recent fault. The former, continuing from western Iran to the north of Bandar Abbas; towards northwest, the border structure, consists of a sum of right- handed strike- slip faults, called main recent fault (Tchalenko and Braud, 1974). Strong earthquakes in Zagros mainly happened in different segments of Zagros main recent fault with the dominant direction of northwest- southeast

and dominant consistence of right- lateral strike- slip in the continuation of northeast border (Tchalenko and Braud, 1974).

Regarding the different segments activities of this fault in the western part of Iran, central Iran may show right-lateral strike-slip movement in proportion to Arabia. Different segments of the fault, in Iranian tectonic system are named differently. Dorood, Nahavand, Sahneh and Dinevar parts of Zagros main recent fault have shown more seismic activities in comparison with other parts of the fault, (Sartakht. Morvarid, Marivan and Piranshahr). Geological evidences confirm the right- handed displacement of about 10 to 60 km of the fault in Dorood and Nahavand parts. Earthquake studies pertinent to this fault, indicate their greatness and obvious different mechanisms in comparison with other earthquakes happened in Zagros region, as the dominant mechanism of the earthquakes in this region, is strike- slip or strike- slip with tension component (BHRC, 2006).

One of the most important seismic segments of Zagros main recent fault is Dorood in which one of the most important Iranian historical earthquakes happened, 1909. In Silakhor earthquake (1909), the ground displacement, up to one meter, has pertained to this fault. It forms the southern border of Silakhor in the northwest of Dorood. The segment fault of Dorood, with the direction about N315 and the length of 100km, is the southest fault segment of the present Zagros main fault. Dorood fault is, undoubtedly, the most important and seismic geological structure of this part of the country. Besides the destructive Silakhor earthquake (1909), the ones happened in 1958 and 1962 are pertained to fault as well. (Tchalenko and Braud, 1974).

### 2.3. EARTHQUAKE FOCAL MECHANISM

The focal mechanism of Silakhor earthquake, 31th March 2006, is a right-lateral strike- slip one with normal component, (Fig 2.).

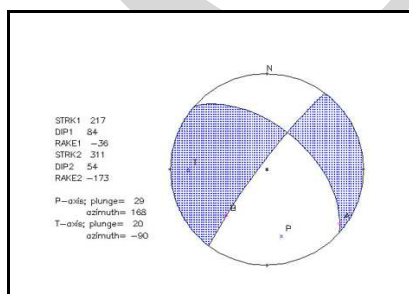


Fig 2. Earthquake focal mechanism based on Harvard site information, 2006.

### 2.3.1. STUDYING THE STRONG GROUND MOTION CAUSED BY THE EARTHQUAKE 31<sup>TH</sup> MARCH , 2006

The seismological engineering characteristics of the main motion have been analyzed based on the seismogram processes represented by Building and Housing Research Center, on the website of the center. The seismograms of Chalanchoolan, Chaghalvandi, KhoramAbad, Samman, Toyserkan, Dorood, Aleshtar and. Stations, 24 stations in total, have been distinguished applicable. The hypocentral distance is evaluated for every seismogram, and the moment magnitude is calculated for each station by using Kanamori, 1977 equation  $M_w$ .

The moment magnitude of this earthquake was  $M_w = 6.0$ , gained by the calculated average of all stations. The maximum acceleration for all three components, concluding horizontal and vertical ones, corner frequency and smoothed level of acceleration fourier spectra for the main shock recorded in 24 accelerographic stations, are calculated and the results are presented in Table 1.

### 2.3.2. SILAKHOR EARTHQUAKE AFTERSHOCKES

Silakhor earthquake, as any other great earthquake, was accompanied by many aftershocks. These aftershocks were recorded in Chalanchoolan, Tooshe-Abesard, Borujerd, Khoramabad, Chaghalvandi and stations. In the earthquake, 31th March 2006, the epicenter was Darb-e-Astane (Silakhor) and its aftershocks are shown in the map (Fig. 3).

This figure shows that the aftershocks are distributed in northwest- southeast direction. Chalanchoolan station is the nearest seismographic station to the earthquake epicenter out of earthquake recorder stations.

Table 1. Calculation of maximum acceleration, corner frequency, smoothed level of acceleration fourier spectrum and moment magnitude (Mw) for 24 accelerographic stations, the recorders of main shock in Silakhor earthquake. Main shock Records of Silakhor Earthquake, 31 th March, 2006 at 01:17:02 (UTC)

No	Station	Record No.	Geog. Coord.		P.G.A (cm/s/s)			Epicer			A0(m/s)	fc(Hz)	R(Km)	Mw
			E	N	H1	V	H2	N	E					
1	Chalan Choolan	4027/08	48.913	33.659	439	522	340	33.74	48.89	0.7	0.4	10	6.1	
2	Chasghalvandi	4018/03	48.553	33.664	179	80	151	33.74	48.89	0.3	0.9	33	5.8	
3	Khoram Abad	4019/02	48.359	33.491	37	17	59	33.74	48.89	0.05	1.3	68	5.3	
4	Samnan	4020/00	48.708	34.21	36	47	57	33.74	48.89	0.1	0.3	60	6.3	
5	Toyserkan	4021/00	48.442	34.552	12	8	13	33.74	48.89	0.03	0.2	106	6.3	
6	Dorud	4022/02	49.095	33.491	34	33	37	33.74	48.89	0.1	0.4	20	5.8	
7	Noor Abad	4024/00	47.972	34.072	47	17	46	33.74	48.89	0.05	0.2	115	6.5	
8	Aleshtar	4025/00	48.246	33.856	155	82	146	33.74	48.89	0.1	0.3	49	6.2	
9	Firoozan	4026/00	48.115	34.36	25	12	22	33.74	48.89	0.02	0.2	123	6.3	
10	Khondab	4028/01	49.154	34.401	52	24	34	33.74	48.89	0.06	1.5	92	5.3	
11	Malayer	4029/00	48.801	34.309	38	35	57	33.74	48.89	0.04	0.2	79	6.3	
12	Giyan	4033/00	48.241	34.172	61	18	28	33.74	48.89	0.08	0.2	95	6.6	
13	Toosh-e-Ab-e-Sard	4035/03	48.569	33.773	326	278	391	33.74	48.89	0.3	1.0	43	5.8	
14	Nahavand	4038/00	48.378	34.186	19	13	26	33.74	48.89	0.04	0.2	88	6.4	
15	Arak	4039/00	49.731	34.101	7	8	11	33.74	48.89	0.03	0.4	76	5.9	
16	Koohdasht	4045/00	47.612	33.524	13	5	10	33.74	48.89	0.04	0.5	98	5.9	
17	Kohnoosh	4050/00	48.278	34.718	14	6	12	33.74	48.89	0.03	0.2	12	5.7	
18	Darreh-Ashar	4052/03	49.06	33.45	105	72	124	33.74	48.89	0.1	0.4	42	6.0	
19	Sefid Dasht	4053/00	48.891	33.218	21	18	21	33.74	48.89	0.6	0.9	49	6.1	
20	Shazand	4054/01	49.406	33.931	26	20	21	33.74	48.89	0.03	0.6	60	5.5	
21	Shool Abad	4055/03	49.192	33.184	40	17	38	33.74	48.89	0.05	0.3	64	6.1	
22	Bahar	4064/00	48.442	34.889	10	6	12	33.74	48.89	0.02	0.2	102	6.2	
23	Qahavand	4065/00	49.002	34.857	14	10	20	33.74	48.89	0.03	0.3	107	6.1	
24	Gonabad	4066/00	48.746	34.682	18	22	24	33.74	48.89	0.05	0.3	65	6.1	

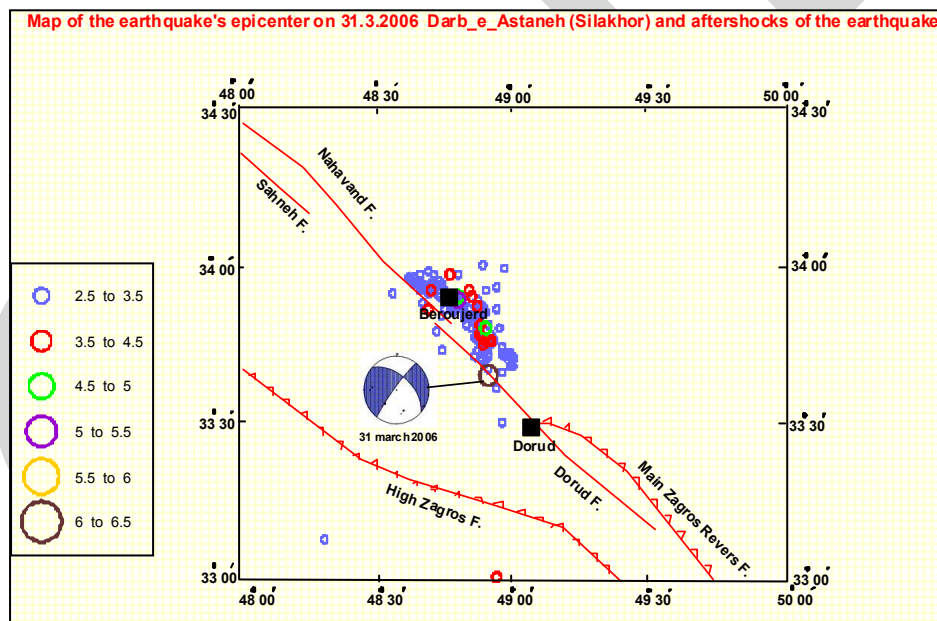


Fig. 3. The epicentral zone of 31.03.2006 earthquake, Darb-e-Astane (Silakhor) and its aftershocks.

**2. 4. STRONG GROUND MOTION IN SILAKHOR EARTHQUAKE**

Silakhor earthquake, 31<sup>th</sup> March 2006 was recorded in Lorestan, Hamedan and central provinces by 15 digital accelerographic instruments, SSA-2. The maximum acceleration, related to Chalanchoolan station and about 522cm/s<sup>2</sup>, was of vertical component. Regarding the greatness of earthquake, geological condition (alluvium) and hypocentral distance (10 km), the recorded acceleration on the vertical component is not unexpected. The maximum

acceleration, recorded at Chalanchoolan station, is 439 cm/s<sup>2</sup> in the horizontal component. The depth of this earthquake is equal to 14 km, according to the report of International Institute of Earthquake Engineering and Seismology (Hamzehloo, 2006). Silakhor earthquake on 31<sup>th</sup> March 2006 was reported and its location was determined by national and international seismographic agencies.

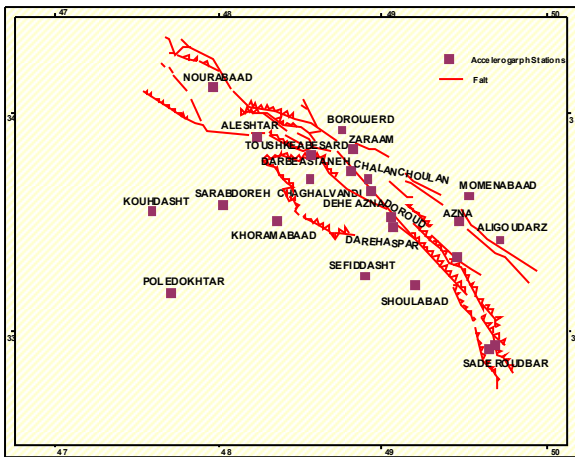


Fig 4. Accelerographic network of Lorestan province

### 3. RESULTS AND DISCUSSION

In this research strong ground motions in Silakhor earthquake 31.03.2006 is studied using Irikura, (1986) method based on experimental Green's function. This method is based on the sub-faults and superposition of the small movements of discrete fractures (subfaults) on the fault plane determined by Irikura simulation law. The azimuth, dip and rake are considered as 311, 54 and 172, respectively, according to Harvard CMT Solution reports. The ruptures distribution in the fault is assumed cyclic (radius). The type of slip function in the fault is selected in the form of ramp based on  $\omega^2$  model (Aki, 1967 & Brune, 1970). The rupture velocity,  $v_r$ , as the percentage of shear wave velocity is determined based on  $v_r = 0.9v_s$  formula. If the waves velocity,  $S$ , is equal to  $3.4 \text{ km/s}$  then, the rupture velocity is  $3 \text{ km/s}$  that has been used. Stress drop for the strong motion generation area is calculated based on the formulation of Madariaga, 1979 and Boatwright, 1988. To calculate stress drop the following formula is used:

$$\Delta\sigma = \frac{7}{16} \frac{M_0}{r^3}$$

where

$r$  is the source radius.

The proportion of the stress drop in great event to that in the small one is gained by:

$$\frac{M_s f_c^r}{M_g f_c^r}$$

The source radius is calculated based on the cyclic source model, using Brune formula (1970);

$$r_0 = \frac{2.34.\beta}{2\pi.f_c}$$

Preciseness in the determination of the needed parameters in simulations is very important for exact evaluation of the ground motions. Another important

factor in the simulations is selecting the aftershocks of proper greatness and high signal to noise ratio. Among 88 aftershock seismograms recorded by Housing Research Center, after being studied, Chalanchoolan, Chaghavandi, Aleshtar and Dorood stations- properly recorded, either mainshock or aftershocks- were selected and simulation were applied to them. The nearest Silakhor earthquake recorder station is Chalanchoolan one in Silakhorregion. According to the results gained by simulation, a proper accordance is seen in comparing the simulated maximum acceleration and the observational ones. In order to control the validity of the method numerically, two parameters-the amplitude proportion,  $a$ , and the remained function,  $r$ - are calculated for each accelerogram, represented in the Table2. The nearer the amplitude proportion is to 1, and also the fewer amount the  $r$  has, the better accordance is seen between the simulated and observational accelerograms. The range of  $r$  differs between 1.8 to 2.3 that is an acceptable range.

Table 2. The calculations related to numerical validity of applied method in modeling

Record No.	Simulated Accelerogram (m/s <sup>2</sup> )	Observational Accelerogram (m/s <sup>2</sup> )	a	r
4018-04(L)	1.59	1.62	1.6	2.2
4018-04(T)	1.15	1.19	1.5	2.2
4018-04(V)	0.39	0.54	0.9	1.8
4018-04(L)	1.31	1.51	1.2	1.9
4018-04(T)	1.28	1.15	0.8	2.1
4018-04(L)	4.38	4.16	0.7	2.1
4018-04(T)	3.45	3.50	0.6	2.3
4018-04(V)	4.77	4.42	0.9	1.9
4018-04(L)	0.37	0.32	0.8	2.0
4018-04(T)	0.30	0.34	0.9	1.9
4018-04(V)	5.08	4.42	0.6	2.0

#### 3. 1. Comparison between the observations and simulations

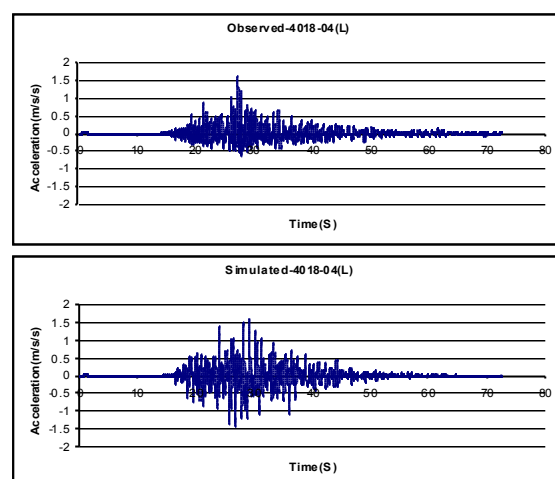


Fig. 5. Comparing the observational accelerogram (a) to the simulated ones (b), based on horizontal component (L) 4018-04 of Chaghavandi station.

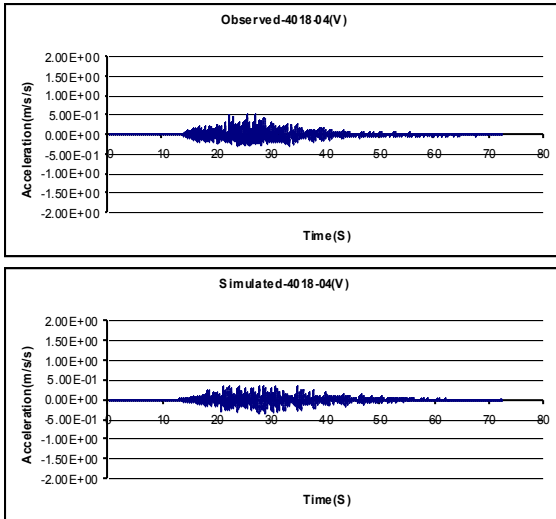


Fig. 6. Comparing the observational accelerogram (a) to the simulated ones (b), based on vertical component (V) 4018-04 of Chaghalvandi station.

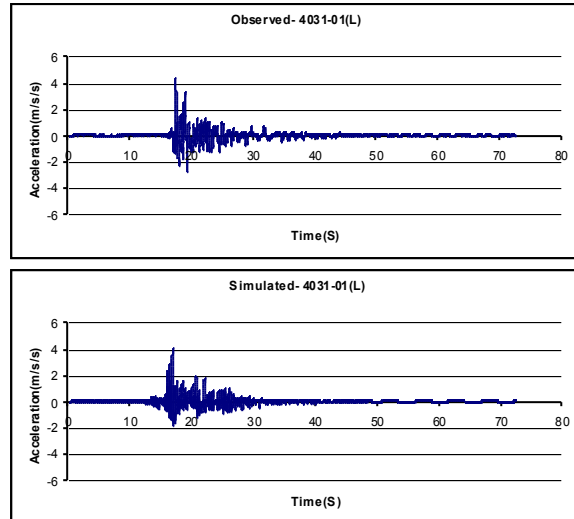


Fig 9. Comparing the observational accelerogram (a) to the simulated ones (b), based on horizontal component (L)4031-01 of Chalanchoolan station.

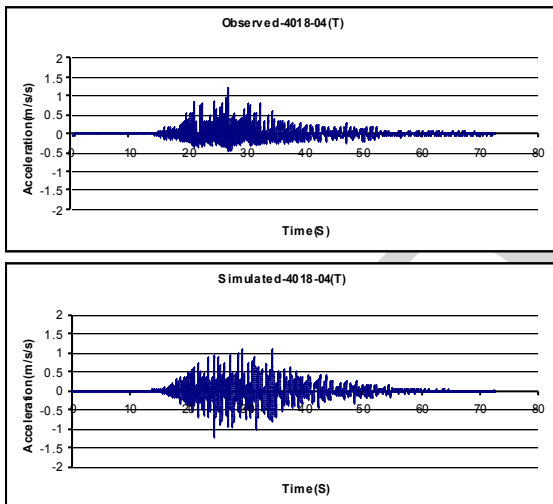


Fig. 7. Comparing the observational accelerogram(a) to the simulated ones(b), based on horizontal component (T)4018-04 of Chaghalvandi station.

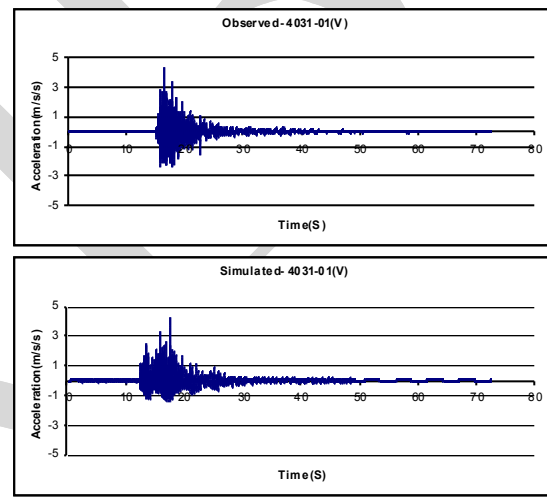


Fig 10. Comparing the observational accelerogram (a) to the simulated ones (b), based on vertical component (V) 4031-01 of Chalanchoolan station.

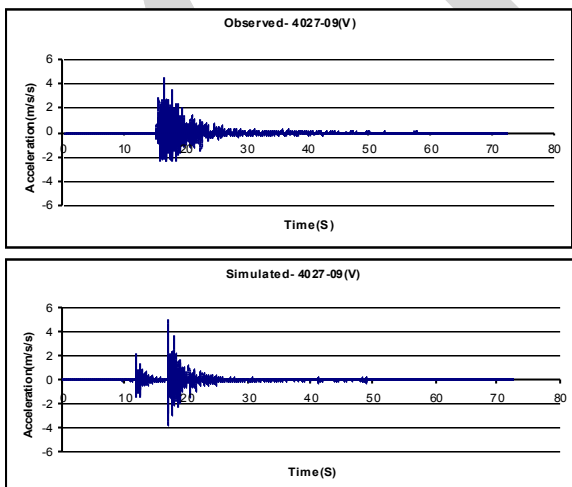


Fig. 8. Comparing the observational accelerogram (a) to the simulated ones (b), based on vertical component (V) 4027-09 of Chalanchoolan station.

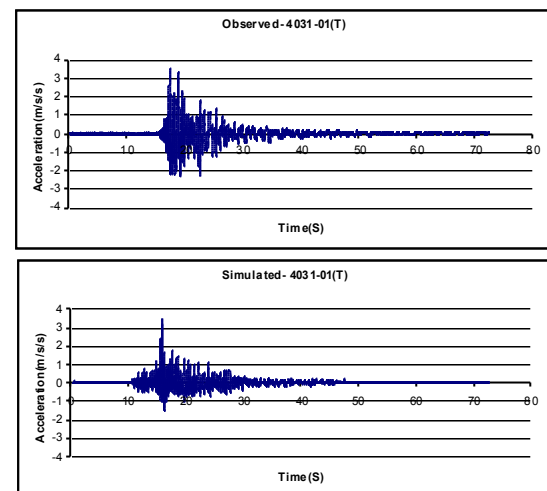


Fig. 11. Comparing the observational (a) to the simulated ones (b), based on horizontal component (T) 4031-01 of Chalanchoolan station.

Studying the simulated spectra, it is observed that these spectra have almost proper accordance with the observational ones of high frequency ranges (over 1 Hz).

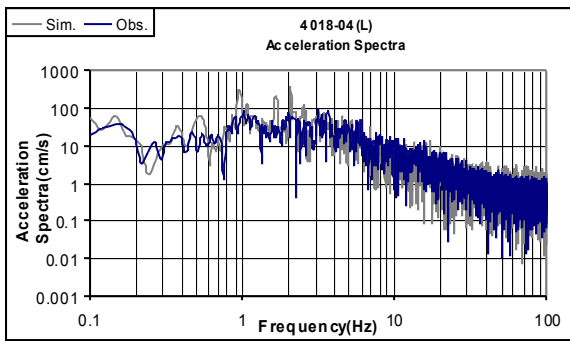


Fig 12. Comparing the simulated acceleration spectra with the observational one 4018-04 (L) of Chaghalvandi station.

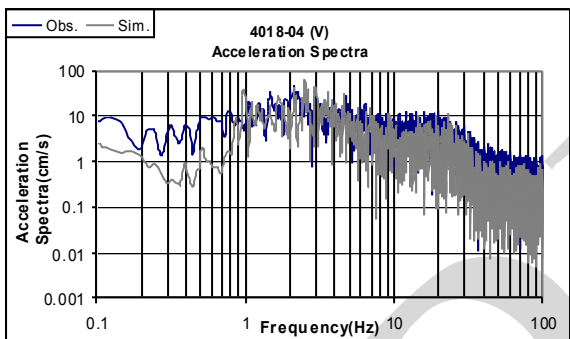


Fig 13. Comparing the simulated acceleration spectra with the observational one 4018-04 (V) of Chaghalvandi station.

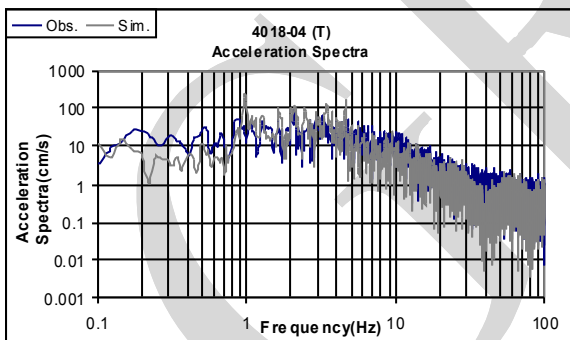


Fig 14. Comparing the simulated acceleration spectra with the observational one 4018-04 (T) of Chaghalvandi station.

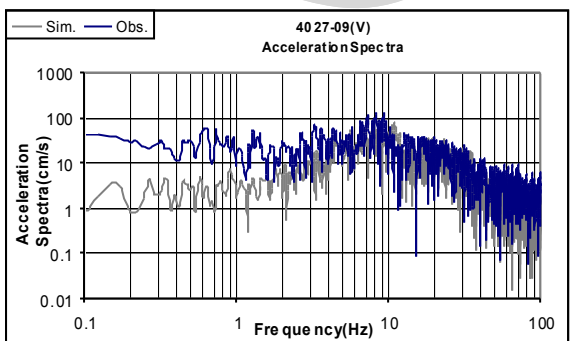


Fig. 15. Comparing the simulated acceleration spectra with the observational one 4027-09 (V) of Chalanchoolan station.

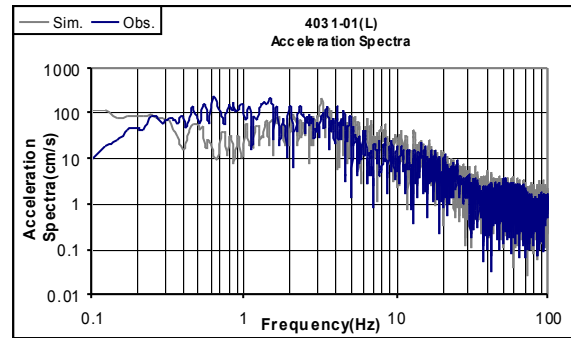


Fig. 16. Comparing the simulated acceleration spectra with the observational one 4031-01 (L) of Chalanchoolan station.

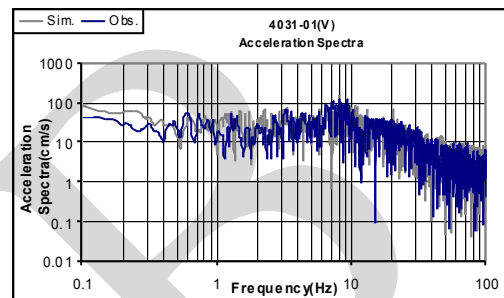


Fig. 17. Comparing the simulated acceleration spectra with the observational one 4031-01 (V) of Chalanchoolan station.

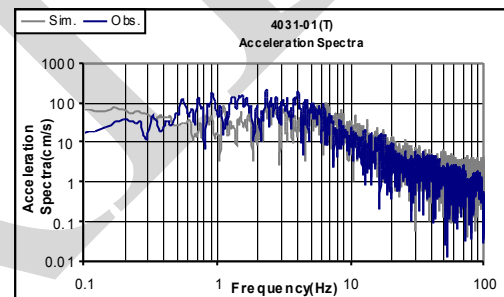


Fig. 18. Comparing the simulated acceleration spectra with the observational one 4031-01 (T) of Chalanchoolan station.

#### 4. CONCLUSION

1. Regarding the results, gained in the simulation, a proper accordance is seen between the simulated maximum accelerations and the observational ones.
2. The selection of the input parameters for simulating, such as: stress drop, rupture starting point, rise time, and ..., has a significant role in the simulating processes, as the maximum acceleration differs according to the parameter selection way; the closeness of the simulated maximum acceleration to the observational one, probably, clarifies the exactness of parameters selection.
3. Studying the simulated acceleration spectra shows that these spectra have almost proper accordance with the observational ones in high frequency ranges (over 1 Hz).
4. Concerning the results gained by acceleration spectra, experimental Green's function method has a high accuracy in the high frequency ranges where the geological heterogeneous structures cannot be

simulated precisely. However, artificial Green's function method- provided by the aid of numerical methods, has a higher accuracy in the low frequency ranges and makes the simulation more precise in this range, as Empirical Green's Function one does not have enough energy here.

5. Among the acceleration fourier spectra simulated at different stations, in Chaghalvandi station (4018-04) - (L), the best and most accordance is seen in the first horizontal component. In other stations, the difference is in the amplitude.

6. The components such as: the second horizontal and the vertical components of Chaghalvandi station (4018-04)-(T, V), the first horizontal component of Chalanchoolan stations (4031-01)-(L), which are fault normal, and also the vertical component of Chalanchoolan station (4027-09)-(V), show no proper accordance (amplitude). They have probably been influenced by the vertical directivity in the vertical component and horizontal component fault normal to the fault.

## REFERENCES

- Hartzel, S.H. (1987) Earthquake Aftershocks as Green's Functions. *Geophysical Research Letters*. 53, 1425 – 1436.
- Irikura, K. (1983) Semi- Empirical Estimation of Strong Ground Motions During large Earthquakes. *Disaster Prevention Research Institute, Kyoto University*, 33 (2), 298.
- Hadley, D.M. & Helmberger, D.V. (1980) Simulation of Strong Ground Motions. *Bulletin Seismology Society American*, 70, 617 – 630.
- Wald, D., Somerville, P.G. & Burdick, L.J. (1988) The Whittier Narrows, California Earthquake of October 1, 1987-Simulation of Recorded Accelerations, Earthquake Spectra. *Earthquake Spectra*, 4 (1), 139 – 156.
- Olson, H.A. & Apsel, J.R. (1982) Finite Faults and Inverse Theory with Applications to the 1979 IMPERIAL VALLEY Earthquake. *Bulletin of the Seismological Society of America*, 72, 1969 – 2001.
- Bour, M. & Cara, M. (1997) Test of a Simple Empirical Green's Function Method on Moderate- Sized Earthquakes. *Bulletin of the Seismological Society of America*, 87, 668 – 683.
- Boore, M. (1983) Stochastic Simulation of High – Frequency Ground Motions based on Seismological Models of the Radiated Spectra. *Bulletin of the Seismological Society of America*, 73, 1865 – 1894.
- Hutchings, L., Stavrakakis, G.N., Ioannidou, E., Francis, T.P. (1997) *Strong Ground Motion Synthesis for a M= 7.2 Earthquake in the Gulf of Corinth, Greece Using Empirical Green's Functions*. This paper was prepared for submittal to the 29<sup>th</sup> IASPEI General Assembly, Thessaloniki, Greece, August 18–28.
- Kamae, K., Irikura, K. & Pitarka, A. (1998) A Technique for Simulating Strong Ground Motion using Hybrid Green's Function. *Bulletin of the Seismological Society of America*, 88, 357– 367.
- Miyake, H., Iwata, T. & Irikura, K. (2003) Source Characterization for Broadband Ground-Motion Simulation, Kinematic Heterogeneous Source Model and Strong Motion Generation Area. *Bulletin of the Seismological Society of America*, 93, 2531 – 2543.
- Miyake, H., Tanaka, Y., Sakaue, M., Koketsu, K. & Ishigaki, Y. (2006) Empirical Green's function Simulation of Broadband Ground Motions on Genkai Island During the 2005 West Off Fukuoka Prefecture Earthquake. *Earth Planets Space*, 58, 1637 – 1642.
- Irikura, K. (1986) *Prediction of Strong Acceleration Motion Using Empirical Green's Function*. Proceeding of the 7<sup>th</sup> Japan Earthquake Engineering Symposium, 151– 156.